





***Ab initio*-based approach for the oxidation mechanisms at SiO₂/4H-SiC interface: Interplay of dry and wet oxidants during interfacial reaction**

Tsunashi Shimizu , Toru Akiyama ,* and Tomonori Ito 
 Department of Physics Engineering, Mie University, Tsu 514-8507, Japan

Hiroyuki Kageshima
 Interdisciplinary Graduate School of Science and Engineering, Shimane University, Matsue 690-8504, Japan

Masashi Uematsu
 Faculty of Science and Technology, Keio University, Yokohama 223-8522, Japan

Kenji Shiraiishi
 Institute of Materials and Systems for Sustainability, Nagoya University, Nagoya 464-8601, Japan

 (Received 18 January 2021; accepted 26 October 2021; published 3 November 2021)

Effects of the coexistence of dry and wet oxidants on the reaction process at SiO₂/4H-SiC(0001) and (000 $\bar{1}$) interfaces during SiC oxidation are systematically investigated by performing *ab initio* calculations. We find characteristic features of the interfacial reaction mechanisms, which are dependent on the plane orientation and wet oxidation condition. The incorporation of wet oxidants leads to lower barrier heights for the reaction of O₂ molecules, resulting in the promotion of interfacial reaction at the SiO₂/4H-SiC(0001) interface. In contrast, the coexisting O₂ molecule assists the reactions by H₂O molecule and OH groups at the SiO₂/4H-SiC(000 $\bar{1}$) interface. Furthermore, we estimate the linear rate constants in the Deal-Grove model using the calculated barrier heights and reveal that the preferable wet ambient condition at the SiO₂/4H-SiC(0001) interface is different from that at the SiO₂/4H-SiC(000 $\bar{1}$) interface. The difference in the rate constants is caused by the difference in the rate-limiting reaction pathway between SiO₂/4H-SiC(0001) and (000 $\bar{1}$) interfaces. These calculated results offer better understanding of the atom-scale mechanisms for the significant enhancement of SiC oxidation by the interplay of dry and wet oxidants.

DOI: [10.1103/PhysRevMaterials.5.114601](https://doi.org/10.1103/PhysRevMaterials.5.114601)

I. INTRODUCTION

Silicon carbide with 4H structure (4H-SiC) has superior physical properties such as high thermal conductivity and a high breakdown field, which is promising for applications in power electronics devices. Moreover, the ability to form silicon dioxide (SiO₂) by thermal oxidation similar to Si is advantageous for fabricating metal-oxide-semiconductor field-effect transistors (MOSFETs) compared with other wide-gap semiconductors. However, the degradation in performance of SiC-MOSFETs such as channel mobility is caused by high interface trap density (D_{it}) near the interface between SiO₂ and 4H-SiC (SiO₂/4H-SiC) [1,2]. It has been suggested that carbon-related defects are the most likely physical origin of D_{it} [2].

To produce high-quality SiO₂/4H-SiC interfaces and manufacture high-performance SiC power devices, many experimental studies using Auger electron spectroscopy [3], ellipsometry [4–12], secondary ion mass spectroscopy [13,14], $C - V$ measurements [8,11,12,14–19], $I - V$ measurements [19,20], thermogravimetric technique [21], Rutherford

backscattering spectroscopy [5], Fourier transform infrared spectroscopy [22–26], grazing incident x-ray reflectivity [17,26,27], x-ray photoelectron spectroscopy [3,17,23,25], atomic force microscopy [17], electron spin resonance [28], and transmission electron microscopy [28], as well as theoretical analysis on the basis of *ab initio* calculations [29–39], diffusion equations [40,41], and molecular dynamics simulations [28,42] have been carried out to clarify the thermal oxidation mechanisms. Furthermore, Harris and Afanasev [43] and Vickridge *et al.* [44] reviewed the experimental studies for the nature of thermal oxide and of the SiO₂/SiC interfaces. According to experimental studies, it is well-known that the oxidation rate of SiC on the Si-face SiC(000 $\bar{1}$) surface is much higher than that on the C-face SiC(0001) surface [3–5,7,8,10,13,15,16,23,27]. From the slope of Arrhenius plots of the growth rate as a function of temperature, the activation energies have been estimated to be 2.3–3.8 and 2.1 eV on the SiC(0001) and (000 $\bar{1}$) surfaces in dry (O₂) ambients, respectively [9,12,17,27]. For wet (H₂O) ambients, the activation energies have been estimated as 2.8–3.0 and 2.3 eV on the on the SiC(0001) and (000 $\bar{1}$) surfaces, respectively. [9,25] To explain the experimental results, several models [5–8,11,40] on the basis of the Deal-Grove model [45] have been proposed for the oxide growth of SiC. More

*akiyama@phen.mie-u.ac.jp

recently, it is known that the introduction of an O_2 molecule into wet ambient crucially affects the interface properties. The channel mobility improvement and D_{it} reduction in MOSFETs by using a wet ambient have been demonstrated from $C - V$ measurements [5,14,20]. The instability of threshold voltage by wet oxidation has been induced by the gate bias stressing in SiC-MOS devices [16]. According to these experimental findings, much attention has been paid to the control of the oxidation ambient to improve the interface qualities. More importantly, $C - V$ measurements in addition to infrared absorption spectroscopy measurements have demonstrated that the coexistence of dry and wet oxidants contributes to the improvements of electrical properties in MOS capacitors [24–26]. Furthermore, it has been clearly observed that the coexistence of H_2O and O_2 leads to a significant enhancement of interfacial reaction processes [25,26,46]. The enhancement of interfacial reaction is quite different from the case of thermal oxidation of silicon, in which the growth rate monotonically increases with the ratio of H_2O in an oxidizing ambients [47]. However, microscopic understanding of the enhancement caused by coexisting dry and wet oxidants at the interface is still lacking.

Previously, we performed calculations for the reactions during dry and wet thermal oxidations at $SiO_2/4H-SiC(0001)$ and $(000\bar{1})$ interfaces on the basis of *ab initio* calculations [35,36]. We reported that for dry oxidation the desorption of CO molecules stabilizes newly formed SiO_2 , while the formation of $Si-O-CH_2-C$ and $Si-CH-OH$ bonds does the interface after the reaction by wet oxidants. We have also proposed the variation of atomic structure during the O_2 reaction including wet oxidants such as H_2O molecule and OH groups at $SiO_2/4H-SiC(0001)$ and $(000\bar{1})$ interfaces [37]. For the $SiO_2/4H-SiC(0001)$ interface, there is little contribution of the H_2O molecule and single OH group to the O_2 reaction leading to the desorption of CO molecule. The stable interface is obtained with the desorption of the CO_2 molecule after the reaction of both the O_2 molecule and two OH groups. In contrast, not only the O_2 molecule but also the H_2O molecule and OH groups easily react and stabilize the interface with CO_2 formation at the $SiO_2/4H-SiC(000\bar{1})$ interface. In addition to the energetics of the oxidants near the interface, we have suggested a possible reaction process where the coexistence of H_2O and O_2 molecules contributes at the $SiO_2/4H-SiC(000\bar{1})$ interface [38]. In spite of these findings, physical origins of significant enhancement of interfacial reaction have never been clarified from theoretical viewpoints.

In this paper, we focus on the effect of coexisting oxidants on the interfacial reaction because the reaction process at the interface is dominant for the growth rate of thin oxides (less than 50 nm) for SiC MOSFETs, as pointed out by the Deal-Grove model [45]. To clarify the behavior of coexisting dry and wet oxidants at the $SiO_2/4H-SiC$ interface, the interfacial reaction pathways for the concerted mechanism of wet oxidants such as the H_2O molecule and OH groups with O_2 molecule are systematically investigated by performing *ab initio* calculations. In addition to *ab initio* calculations, the underlying physics and chemistry of the oxide growth enhancement depending on the orientation and wet oxidation condition are discussed based on the analysis of linear rate constants in the Deal-Grove model. The effect of wet oxida-

tion ratio with respect to the dry oxidants are evaluated by the analysis of linear rate constants using the calculated energy barriers obtained by *ab initio* calculations. The rest of this paper is organized as follows. In Sec. II, we briefly describe computational procedures including calculation models. In Secs. III A and III B, the calculated results for the reactions at $SiO_2/4H-SiC(0001)$ and $(000\bar{1})$ interfaces are discussed, respectively. Section III C is devoted to discuss the orientation and wet oxidation condition dependence. In Sec. IV, we conclude our findings.

II. METHODOLOGY

To simulate isolated $SiO_2/4H-SiC$ interfaces away from the bulk region of SiC and SiO_2 surfaces, we employ slab models whose bottom and top surfaces are terminated by H atoms [48]. For both $SiO_2/4H-SiC(0001)$ and $(000\bar{1})$ interfaces, the $c(2\sqrt{3} \times 3)$ slab models with four 4H-SiC bilayers and two SiO_2 monolayers are used. A vacuum region of 10 Å thickness, which is enough to eliminate the interactions between adjacent slabs, is included in the unit cells of slab models. As a representative of SiO_2 generated by thermal oxidation of SiC, SiO_2 with a cristobalitelike structure is adopted. Intrinsic defects in SiO_2 and those on the SiC side of the interface [2,24,49,50] are not included in the slab models considered in this paper. By using present slab models, similar atomic configurations at $SiO_2/4H-SiC$ interfaces to those reported in previous calculations are successfully obtained [29,30,32]. Since amorphous SiO_2 is formed by the thermal oxidation of SiC, the nature of disordered SiO_2 is occasionally crucial for the behavior of additional atoms and molecules in SiO_2 [51–54]. However, it is likely that the oxidizing species such as O_2 and H_2O molecules located in the opening space of SiO_2 directly attaches the topmost layer of SiC during the interfacial reaction. Although effects of disordered SiO_2 should be carefully verified, plausible reaction pathways of oxidizing species at the interface could be achieved even by present ordered interface models. Indeed, the calculated barrier height of O_2 molecule at SiO_2/Si interface with ordered SiO_2 [55] agrees well with those using the interface with amorphous SiO_2 [56], where the O_2 molecule directly attaches the Si substrate and dissociates into Si–O bonds. It is also confirmed that SiO_2 density in our slab models is 2.2 g/cm³, comparable to that of SiO_2 obtained by Si thermal oxidation. The atoms belonging to the bottom bilayer are fixed at their ideal positions.

Ab initio calculations are performed using the extended Tokyo *Ab initio* Program Package (xTAPP), which is based on density functional theory with pseudopotentials and a plane-wave basis set [57,58]. For the exchange-correlation energy among electrons, a form by the Perdew-Burke-Ernzerhof functional within the generalized gradient approximation (GGA-PBE) including spin degrees of freedom is used [59]. We use ultrasoft (norm-conserving) pseudopotentials to describe the interactions between electrons and ions for C and O (Si and H) atoms [60,61]. The validity of these pseudopotentials has been verified in our previous study [35]. The valence wave functions are expanded by the plane-wave basis set. The cutoff energies for the wave functions and charge densities are 30.25 and 121 Ry, respectively. The conjugate-gradient

method is utilized for both electronic-structure calculations and geometry optimization [62,63]. According to the additional calculations using a vacuum region of 20 Å thickness with wave-function cutoff energy of 64 Ry, we have confirmed that the errors caused by the calculation condition such as vacuum region and cutoff energies are less than 0.02 eV. The errors within 0.02 eV are acceptable in the evaluation of energies in this paper.

To evaluate the reaction of the oxidants, we here introduce the reaction energy E_{rc} , which is simply calculated from the total-energy difference between the initial and final interface structures. The effect of translational, vibrational, and rotational entropy of molecules is not accounted for the reaction energy. This is because the energy range of E_{rc} (~ 8.2 eV) [37,38] is much larger than the chemical potentials of molecules including translational, vibrational, and rotational motions even at high temperatures. Furthermore, as described in Secs. III A and III B, either CO or CO₂ molecule is formed in the final-state structures and the entropy of molecules in the initial-state structure cancels out that in the final-state structure. Although the GGA-PBE overestimates the binding energy of O₂ molecule by 0.7 eV, the values of E_{rc} are insensitive to the choice of exchange-correlation functionals. The calculations using the revised version of GGA (revPBE) [64], which gives more accurate binding energies of molecules, reveal that E_{rc} in the GGA-PBE is smaller than that in the revPBE by ~ 0.09 eV. It is therefore indicated that the qualitative trend for the reactions of molecules at the interface can be obtained within the GGA-PBE calculations. In this paper, a single O₂ molecule in triplet state as dry oxidant and either H₂O molecule or OH groups as wet oxidants during the interfacial reaction are considered. The consideration of OH groups is based on the observations of infrared peaks originating from silanol (Si–OH) bands in SiO₂ [65] and the possibilities of H₂O dissociation resulting in the OH groups, which have been proposed by *ab initio* calculations [66,67]. The experimental results have definitely supported the presence of OH groups as well as the H₂O molecule in SiO₂ [65]. Furthermore, *ab initio* calculations have demonstrated small formation energies of OH groups and low barrier heights for H₂O dissociation in SiO₂ [66,67]. We assume that OH groups are generated by the dissociation of H₂O in SiO₂ and they act as one of oxidizing species at the interface. The effect of the remaining H atoms from the H₂O dissociation on the interfacial reaction is not considered in the present paper.

To search the reaction pathways and barrier heights, we furthermore apply the nudged elastic band (NEB) technique [68]. The minimum energy path along the reaction coordinate r_c is constructed to evaluate the barrier heights. Here, r_c is calculated by the summation of atomic displacements between n th atomic coordinates $\{\mathbf{R}_i^n\}$ labeled by atom index i and $(n+1)$ th atomic coordinates $\{\mathbf{R}_i^{n+1}\}$ as $r_c = \sum_i |\mathbf{R}_i^{n+1} - \mathbf{R}_i^n|$. For the initial-state structures in the NEB calculations, we use the structures of oxidizing species in the SiO₂ region of the interface, which have been obtained in our previous studies [37,38]. For determining the final-state structures in the NEB calculations, we perform an extensive search for stable structures. For each reaction species, we consider ~ 25 initial atomic configurations and perform the geometry optimization. Although a number of reaction pathways are possible, several

plausible reaction pathways are explored by the NEB calculations using stable and metastable structures as final-state structures. The stable and metastable structures for the NEB calculations are simply selected on the basis of E_{rc} . For each reaction species, in addition to the NEB calculations using the most stable structure with the largest E_{rc} in the final state, the NEB calculations are performed using metastable structures whose reaction energy are smaller than that of the most stable structure within ~ 1.2 eV.

III. RESULTS AND DISCUSSION

A. Reactions by coexisting dry and wet oxidants at SiO₂/4H-SiC(0001) interface

We have previously investigated the effects of wet oxidants (H₂O molecule and OH groups) at the SiO₂/4H-SiC(0001) interface [37]. From the energetics of the interface, it has been found that wet oxidants with the form of a H₂O molecule and single OH group are not active at the SiO₂/4H-SiC(0001) interface. The desorption of CO molecules occurs by the incorporation of O₂ molecules, but wet oxidants are left in the SiO₂ region. Although another stable interface structure with H₂O dissociation into the OH group and H atom is found in this study [69], the calculated barrier height (2.65 eV) is too high to promote the interfacial reaction. Furthermore, if we account for the chemical potentials of ideal gas for O₂, H₂O, and CO molecules in the initial and final structures at high temperatures around 1400 K [70], the sum of chemical potentials of O₂ and H₂O molecules in the initial state is lower than that of the CO molecule in the final state by 4.0 eV at 760 Torr, and the difference between the sum of O₂ and H₂O chemical potentials and CO chemical potential becomes large with decreasing pressure. Although the energy of the final state without taking account of the chemical potentials is 1.19 eV lower than that of initial state, the free energy of the initial state becomes lower than the free energy of the final state at high temperatures, indicating that the reaction of coexisting O₂ and H₂O molecules hardly occurs. In the case of the reaction by O₂ molecule and single OH group, the calculated barrier height (3.89 eV) is found to be much higher than those of O₂ molecules. It is thus implied that the contribution of a single OH group is negligible to the interfacial reaction of a O₂ molecule.

In contrast, our calculations demonstrate that the coexistence of the O₂ molecule and two OH groups leads to different atomic configurations from those obtained by previous calculations [37]. Indeed, the reaction to form atomic configurations is decisive to understand the significant enhancement of interfacial reaction by the coexistence of dry and wet oxidants at the SiO₂/4H-SiC(0001) interface. Figure 1 shows the initial and final states for the reaction of the O₂ molecule and two OH groups (O₂ + 2OH reaction) obtained by present calculations. As shown in Fig. 1(a), weak bonds are formed between OH groups and Si atoms of SiO₂ in the initial-state structure. Therefore, OH groups can be regarded as charged OH[−], owing to the charge transfer between O and Si atoms. The bond length of Si–OH (~ 1.74 Å) shown in Fig. 1(a) is larger than those in Si–O bonds in host SiO₂ (~ 1.66 Å) and the Lowdin charges of O atoms in Si–OH

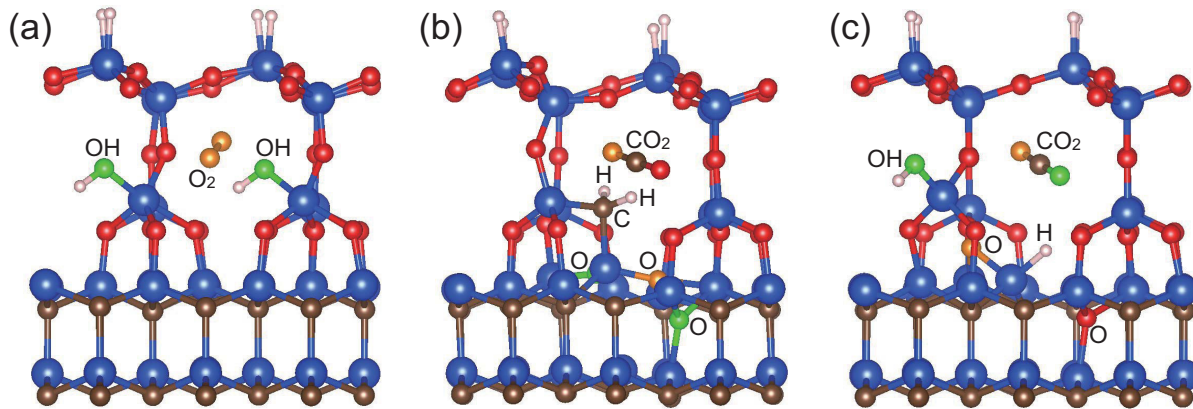


FIG. 1. Side views of (a) O_2 and two Si–O–H bonds in SiO_2 region as an initial state, and (b) CO_2 with Si– CH_2 –Si bond and (c) CO_2 with Si–O–H and Si–H bonds as final states for the reaction of O_2 molecule and two OH groups ($O_2 + 2OH$ reaction) at the $SiO_2/4H-SiC(0001)$ interface. Si, C, O, and H atoms are represented by blue, brown, red, and pink circles, respectively. O atoms of dry oxidant (O_2 molecule) are displayed by orange circles, and those of wet oxidants (H_2O and OH groups) are displayed by green circles. Note that the H atoms of top surface are used to terminate Si dangling bonds of SiO_2 .

(6.47) are smaller than those of Si–O bonds in SiO_2 (6.81). As a metastable structure for the final state of the $O_2 + 2OH$ reaction, the CO_2 molecule and Si– CH_2 –Si bond [Fig. 1(b)] are formed and its reaction energy is 6.21 eV. The stable structure for the $O_2 + 2OH$ reaction shown in Fig. 1(c) is composed of Si–O–H and Si–H bonds with CO_2 molecules. This atomic configuration is close to the resultant structure for the O_2 reaction with the single OH group [69]. The calculated E_{rc} for this structural change (7.08 eV) is higher than those obtained by previous calculations [37].

From the NEB calculations, the structural changes different from those of the single oxidation process by dry and wet oxidants are found in the processes to form the structures shown in Figs. 1(b) and 1(c). Figure 2(a) shows the energy variation and structural change along the reaction pathway of O_2 molecule in triplet state with two OH groups to form a Si– CH_2 –Si bond with CO_2 desorption. Two OH groups move toward the SiO_2 region, and O–O–H and new Si–O–H bonds are formed as a metastable state [C in Fig. 2(a)]. After the O–

H bond formation, the O atom of OH group is incorporated into the SiC substrate, along with the formation of Si–O–C and Si₂–O–H bonds [E in Fig. 2(a)]. The barrier height for these structural changes is 1.07 eV, which corresponds to the dissociation of the OH group. The O_2 molecule and remaining OH group move toward the interface and the formation of Si–O–CO–Si and Si–CH–OH bonds shown in G of Fig. 1(a) occurs simultaneously. The energy of the interface composed of Si–CH–OH and Si–O–CO–Si bonds is 3.24 eV lower than that of the initial state. The calculated barrier height to form Si–CH–OH and Si–O–CO–Si bonds is 1.79 eV. After the formation of Si–CH–OH and Si–O–CO–Si bonds, the dissociation of the Si–CH–OH bond into the Si– CH_2 bond occurs and O atom induces the desorption CO_2 molecule from CO group of Si–O–CO–Si bonds. The CO_2 molecule is finally generated in SiO_2 region with Si– CH_2 –Si bond [I in Fig. 2(a)]. The energy increase from G to H in Fig. 1(a) is due to the dissociation of Si–C and C–O in the Si–O–CO–Si bond, so a large energy gain of 6.26 eV from H to I in Fig. 1(a) is

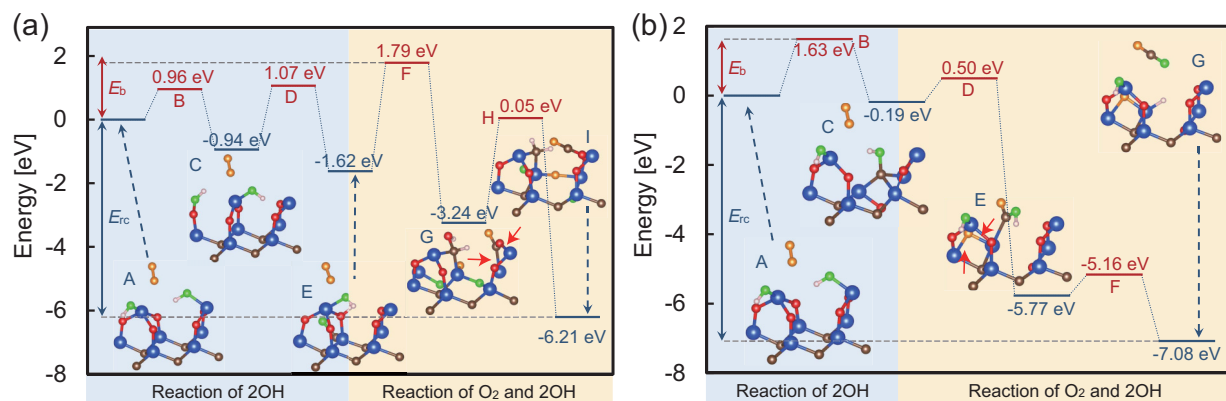


FIG. 2. Energy variation and structural change for the reaction leading to the formation of (a) Si– CH_2 –Si bonds with CO_2 desorption and (b) Si–O–H and Si–H bonds with CO_2 desorption from O_2 and two OH groups. Initial, transition, metastable, and stable states are labeled by A–I. Transition states are depicted in red levels while initial, metastable, and final states are represented by blue levels. For the geometries, the same notation as Fig. 1 is used to specify the atomic species. Red arrows represent Si–C and C–O bonds in the Si–O–CO–Si and Si–O bonds of the Si₃–O (three Si–O). Note that only a part of the unit cell is shown in the structural change.

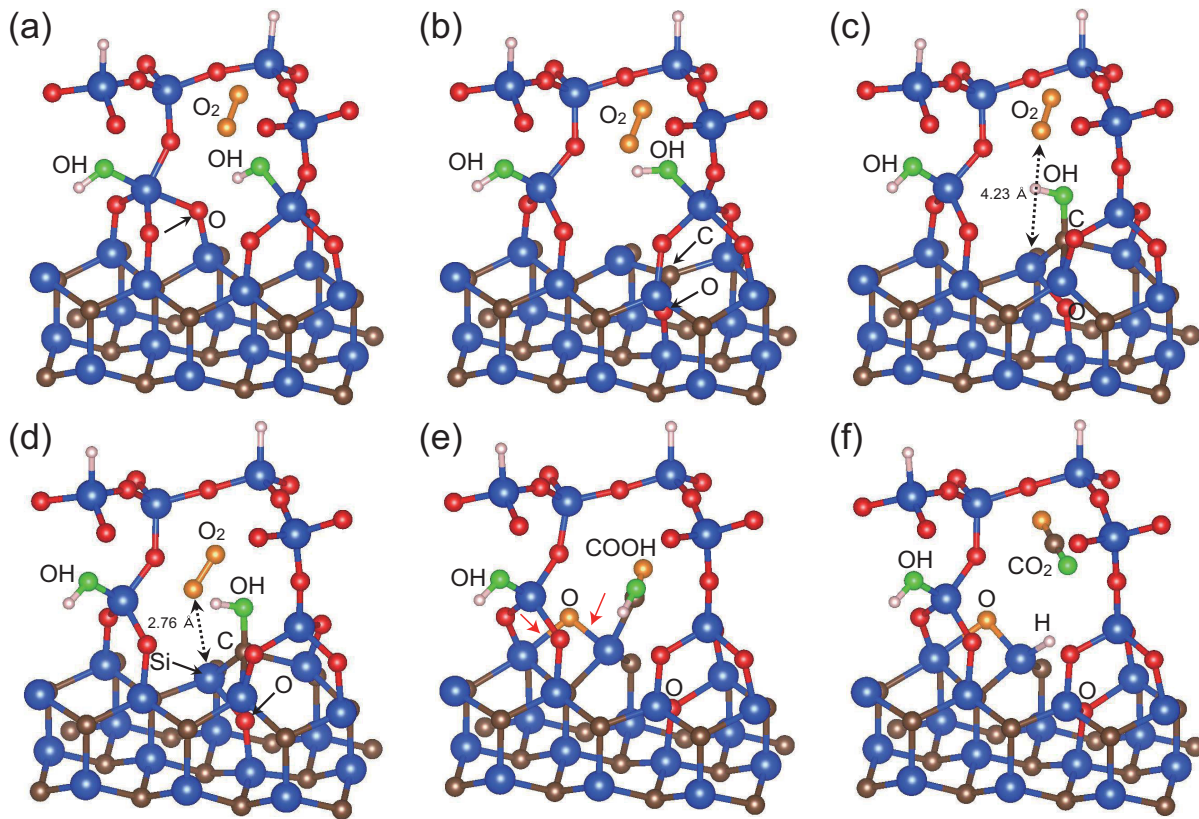


FIG. 3. Structural change for the $O_2 + 2OH$ reaction at the $SiO_2/4H-SiC(0001)$ interface. Perspective views of (a) O_2 in SiO_2 region with two $Si-O-H$ bonds, (b) O_2 and two $Si-O-H$ bonds in SiO_2 region, and $Si-O-C$ bonds at the interface, (c) O_2 and $Si-O-H$ bonds in SiO_2 region, and $Si-O-Si$ and $C-OH$ bonds at the interface, (d) transition state for $Si-O-H$, Si_3-O , $Si-COOH$ bonds formation, (e) $Si-O-H$ bond in SiO_2 region and two Si_3-O and $Si-COOH$ bonds at the interface, and (f) $Si-O-H$ bonds and CO_2 in SiO_2 region and two Si_3-O bonds at the interface, are displayed. The same notation as Fig. 1 is used to specify the atomic species. Red arrows represent $Si-O$ bonds of the Si_3-O . Note that the H atoms of top surface are used to terminate Si dangling bonds of SiO_2 .

caused by the high-energy transition-state structure shown in I of Fig. 1(a). Therefore, the barrier height for the structural change to form $Si-CH_2-Si$ bonds with CO_2 molecules shown in Fig. 2(a) is 1.79 eV, which is lower than those of dry and wet oxidations (3.2 and 2.2 eV, respectively) [35,36].

Figure 2(b) shows the energy variation and structural change for the structural change to form $Si-O-H$ and $Si-H$ bonds with CO_2 desorption shown in Fig. 1(c). Similar to the reaction process of the O_2 molecule with the single OH group ($O_2 + OH$ reaction) [69], one OH group preferentially moves toward the SiC substrate and the $C-OH$ bond is formed as shown in Fig. 3(c) and C of Fig. 2(b). The calculated barrier height for this structural is 1.63 eV, which corresponds to the formation of the transition state shown in Fig. 3(b) and B of Fig. 2(b). The transition state consists of the $Si-O-C$ bond from the incorporation of O atom described by arrow in Fig. 3(a). After the $C-OH$ bond formation, the O_2 molecule moves toward the interface and the $Si-COOH$ bond is formed as shown in Fig. 3(e) and E of Fig. 2(b) by way of the transition transition state shown in Fig. 3(d) and D of Fig. 2(b). It should be noted that a significant energy gain of 5.58 eV from the $C-OH$ bond shown in C of Fig. 2(b) and Fig. 3(c) to the $Si-COOH$ bonds in E of Fig. 2(b) and Fig. 3(e) originates from the generation of new $Si-O$ bonds of the Si_3-O [three $Si-O$, red arrows in Fig. 3(e)]. Since the distance between the

O atom of O_2 molecule and the topmost Si atom of SiC (2.76 Å) in the transition state [dashed arrow in Fig. 3(d)] is smaller than that in the metastable state (4.23 Å) shown by arrow in Fig. 3(c), the barrier height of 0.5 eV corresponds to the dissociation of O_2 molecule by the topmost Si atom [55,56]. In addition to the dissociation of O_2 molecules, the $Si-COOH$ and Si_3-O bonds shown in Fig. 3(e) are formed by the dissociation of $Si-O$ bonds between the Si and O atoms [solid arrows in Fig. 3(d)]. Finally, the formation of $Si-H$ bond with CO_2 desorption easily occurs, as shown in Fig. 3(f) and G of Fig. 2(b).

The calculated barrier height for a set of the reactions to form the structure shown in Fig. 1(c) is 1.63 eV, corresponding to the dissociation of $Si-O-Si$ and $Si-C$ bonds and the formation of $C-O$ bond shown in Fig. 3(b) and B of Fig. 2(b). The value of barrier height is much lower than those of the single oxidation reactions by dry and wet oxidants [35,36]. This is because the initial reaction of OH group forming the $C-OH$ bond generates a Si dangling bond. Comparing the calculated result shown in Fig. 2(b) with that shown in Fig. 2(a), the barrier height for the reaction shown in Fig. 2(b) is lower than that shown in Fig. 2(a), and the reaction energy shown in Fig. 2(b) is larger than that shown in Fig. 2(a). It is thus concluded that the $O_2 + 2OH$ reaction resulting in the CO_2 desorption with $Si-O-H$ and $Si-H$ formation shown in Fig. 2(b) is most likely

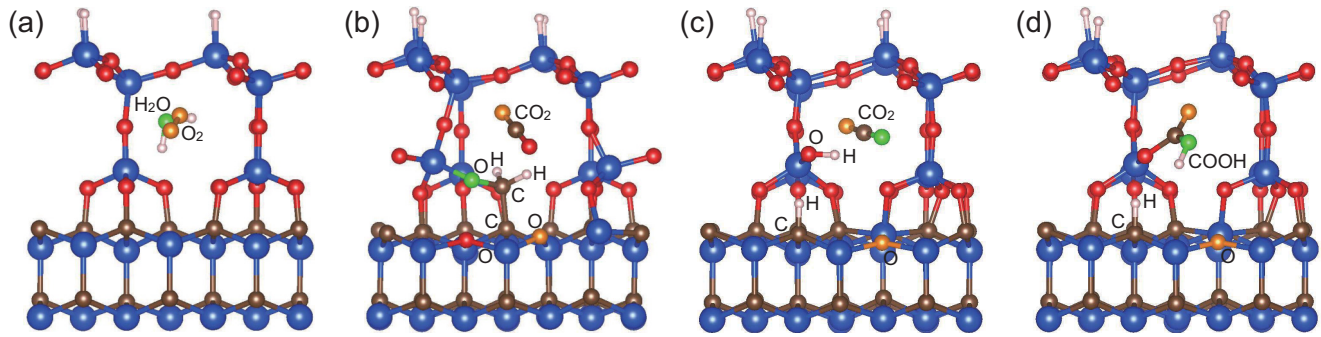


FIG. 4. Side views of (a) O_2 and H_2O in SiO_2 region as an initial state, (b) CO_2 with $Si-O-CH_2-C$ bonds, (c) CO_2 with $Si-O-H$ and $Si-C-H$ bonds, and (d) $Si-C-H$ and $Si-O-COOH$ bonds as final states for the $O_2 + H_2O$ reaction at the $SiO_2/4H-SiC(000\bar{1})$ interface. The same notation as Fig. 1 is used to specify the atomic species. Note that the H atoms of top surface are used to terminate Si dangling bonds of SiO_2 .

to occur at the $SiO_2/4H-SiC(0001)$ interface. Furthermore, the barrier height for the $O_2 + 2OH$ reaction is much lower than E_b with H_2O molecule and single OH group (2.65 and 3.18 eV, respectively) [69]. The difference in E_b depending on the type of wet oxidant implies that the presence of a number of OH groups at the interface contribute to the promotion of O_2 reactions at the $SiO_2/4H-SiC(0001)$ interface.

On the basis of calculated results for the O_2 reaction with H_2O and OH groups, we comment on the effects of a mixed ambient of dry and wet oxidants on the interfacial reaction at $SiO_2/4H-SiC(0001)$ interfaces. Focusing on the barrier height for the O_2 reaction, the barrier heights for O_2 dissociation in the $O_2 + 2OH$ reaction shown in Fig. 2(b) is 0.69 eV, whereas those in the $O_2 + H_2O$ and $O_2 + OH$ reactions are 1.09 and 2.16 eV, respectively [69]. These values are much lower than that of O_2 molecules during dry oxidation (3.2 eV), suggesting the incorporation of either the H_2O molecule or OH groups certainly contributes to the reduction of barrier height for the dissociation of the O_2 molecule. As shown in Fig. 1(c), many topmost carbon lattice sites of SiC, which can be replaced by the O atoms of oxidant, still remain at the interface. It is therefore likely that the reduction of barrier height for the O_2 reaction by OH groups continues after the reactions obtained by present calculations. From the viewpoint of defect generation at the interface, it is expected that the formation of C-related defects is suppressed by the CO_2 formation resulting from the concerted reactions shown in Fig. 3(f) and G of Fig. 2(b). Furthermore, we can expect that H atoms contribute the passivation since the H atom from H_2O molecule terminates the dangling bond of the topmost Si atom of SiC.

B. Reactions by coexisting dry and wet oxidants at $SiO_2/4H-SiC(000\bar{1})$ interface

For the $SiO_2/4H-SiC(000\bar{1})$ interface, we have previously revealed that a wet oxidant such as an H_2O molecule easily reacts at the interface by the coexisting O_2 molecule [37] and the reaction of the H_2O molecule initially occurs as an initial reaction forming $Si-O-CH_2-C$ bonds [38]. In this paper, we find another initial reaction by the O_2 molecule leading to the metastable state with the CO desorption. In this case, the metastable state with the CO molecule is stable compared to the interface with $Si-O-CH_2-C$ bond formation in Ref. [37].

Here, we discuss which reaction pathway is preferentially chosen by the mixture of O_2 and H_2O molecules. Figure 4(a) shows the structure of both O_2 and H_2O molecules coexisting in the SiO_2 region, which is considered as an initial state for the reaction. The reaction of the H_2O molecule leads to the formation of $Si-O-C$ bonds with the CO_2 desorption shown in Fig. 4(b). On the other hand, if we assume the reaction of the O_2 molecule prior to the reaction of the H_2O molecule, the geometry composed of $Si-O-H$ and $Si-C-H$ bonds and CO_2 molecules shown in Fig. 4(c) is also found as a possible candidate for final states for the $O_2 + H_2O$ reaction. These types of bond formation ($Si-O-CH_2-C$ bond or $Si-O-H$ and $Si-C-H$ bonds) have been suggested as stable structures during wet oxidation in previous calculations [38]. Furthermore, the $Si-O-COOH$ bond shown in Fig. 4(d) is found to be formed instead of the $Si-O-H$ bond and CO_2 molecule. The calculated E_{rc} for the structure shown in Fig. 4(d) is only 0.03 eV higher than that shown in Fig. 4(c). This suggests that the $Si-O-COOH$ bond formation occurs as well as CO_2 desorption, so the geometry to form $Si-O-COOH$ and C-H bonds shown in Fig. 4(d) can be considered as a possible final state.

Figure 5(a) shows the energy variation and structural change for the structural change to form the structure shown in Fig. 4(b). During the structural change to form the structure shown in Fig. 4(b), the H_2O molecule initially moves toward the interface and the $Si-O-CH_2-C$ bond is formed from the dissociation of the H_2O molecule [E in Fig. 5(a)]. After the dissociation of the H_2O molecule, the incorporation of the O_2 molecule in the triplet state leads to the CO_2 desorption [H in Fig. 5(a)] through the $Si-O-CO$ bond formation. The calculated barrier height E_b is 1.51 eV, which corresponds to the formation of the $Si-O-Si$ bond [D in Fig. 5(a)] and the reaction energy E_{rc} is 8.25 eV. Details of the reaction with O_2 and H_2O molecules to form the $Si-O-CH_2-C$ bond and CO_2 molecule at the $SiO_2/4H-SiC(000\bar{1})$ interface have been discussed in previous calculations [38]. An energy gain of 3.7 eV from the $Si-OCH_2-C$ bond and O_2 molecule shown in E of Fig. 5(a) to the $Si-O-CO$ bond shown in G of Fig. 5(a) is due to the formation of new $Si-O$ bonds at the interface [red arrows in G of Fig. 5(a)] with O_2 dissociation [71]. The calculated barrier height for the structural change to form $Si-O-CH_2-C$ bonds with the desorption of the CO_2 molecule

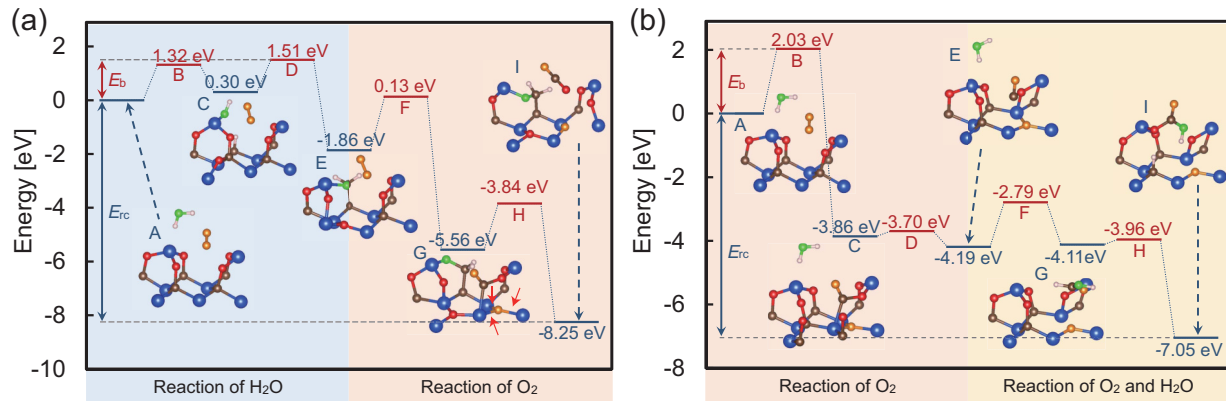


FIG. 5. Energy variation and structural change for the reaction leading to the formation of (a) Si–O–CH₂–C bonds with CO₂ desorption and (b) Si–O–COOH and C–H bonds from O₂ and H₂O molecules. Initial, transition, metastable, and stable states are labeled by A–I. Transition states are depicted in red levels, while initial, metastable, and final states are represented by blue levels. Red arrows represent Si–O bonds of the Si₃–O generated by the dissociation of O₂ molecules. For the geometries, the same notation as Fig. 1 is used to specify the atomic species. Note that only a part of the unit cell is shown in the structural change.

is much lower than those for the single O₂ and H₂O reactions (2.4 and 2.2 eV, respectively) [35,36]. For the structural change to form the atomic configuration shown in Fig. 4(c), the calculated barrier height and E_{rc} are found to be 2.03 and 7.02 eV, respectively. Compared with the reaction shown in Fig. 5(a), the formation of the structure shown in Fig. 4(c) is unlikely to occur due to high E_b and low E_{rc} .

Figure 5(b) shows the energy variation for another O₂ + H₂O reaction leading to the formation of Si–O–COOH and C–H bonds shown in Fig. 4(d). The CO molecule desorbs from the O₂ reaction by way of the transition and metastable states shown in B, C, and D of Fig. 5(b), leading to the formation of the metastable state shown in E of Fig. 5(b). The energy of this atomic configuration is lower than that of the initial state by 4.19 eV. The barrier height for the CO desorption is 2.03 eV, which corresponds to the formation of Si–O–O bonds between SiO₂ and O₂ molecules [B in Fig. 5(b)]. The reaction pathway for the O₂ molecule in the triplet state is similar to the structural change during dry oxidation [35]. After the CO desorption, the H₂O molecule easily reacts with the CO molecule in the SiO₂ region. The formation of the HCOOH molecule occurs by the coalescence of CO and H₂O molecules [G in Fig. 5(b)], and the HCOOH molecule dissociates into the COOH group and H atom (Si–O–COOH and C–H bond formation from Si–O–C bond), leading to the stable structure shown in I of Fig. 5(b). As a result, the barrier height for a set of the reactions shown in Fig. 5(b) is 2.03 eV, which is higher than that for the reaction shown in Fig. 5(a). Although different reaction pathways are found for the O₂ + H₂O reaction, a possible reaction pathway resulting in the enhancement of the interfacial reaction is selected by comparing E_{rc} and E_b . On the basis of low barrier height and large reaction energy shown in Fig. 5(a), the O₂ + H₂O reaction resulting in the CO₂ desorption with Si–O–CH₂–C bond formation shown in Fig. 5(a) is most likely to occur at the SiO₂/4H–SiC(000 $\bar{1}$) interface.

It should be noted that the barrier height for the reaction of each oxidant such as O₂ and H₂O molecules is independent of the sequence of preferentially reacting oxidant. The energy

difference between E and F of Fig. 5(a), which corresponds to the barrier height for the O₂ reaction, is 1.99 eV. This value is similar to the E_b for the O₂ reaction shown in Fig. 5(b). On the other hand, the energy difference between E and F of Fig. 5(b), which corresponds to the barrier height for the reaction of H₂O molecule, is 1.40 eV. This value is only 0.1 eV lower than the barrier height for the H₂O reaction shown in Fig. 5(a).

According to the calculated results for the O₂ + OH and O₂ + 2OH reactions [69], we furthermore find that the barrier heights of the interfacial reaction are reduced by the mixtures of O₂ molecules and OH groups. For the O₂ + OH and O₂ + 2OH reactions, the calculated barrier heights are found to be 1.40 and 1.48 eV, respectively, which are much lower than those for single OH and two OH groups [36]. For the O₂ + 2OH reaction, the desorption of CO caused by wet oxidants in addition to CO₂ desorption is found and a number of C atoms are removed from the topmost layer of SiC substrate. The formation of the interface with CO and CO₂ desorption implies that the coexisting dry and wet oxidants are also effective for the reduction of carbon atoms which cause carbon-related defects at the SiO₂/4H–SiC(000 $\bar{1}$) interface.

On the basis of calculated results for the reaction of wet oxidants with O₂ molecules, we can deduce that the effects of coexisting dry and wet oxidants on the reaction at the SiO₂/4H–SiC(000 $\bar{1}$) interface are different from those at the SiO₂/4H–SiC(0001) interface mentioned in Sec. III A. The calculated barrier height for the reactions shown in Fig. 5(a) (1.51 eV) corresponds to the dissociation of the H₂O molecule. The barrier height is lower than that for wet oxidation (2.2 eV) obtained by previous calculations [36]. In contrast to the SiO₂/4H–SiC(0001) interface, the presence of the O₂ molecule at the SiO₂/4H–SiC(000 $\bar{1}$) interface certainly contributes to the reduction of barrier height in the O₂ + H₂O reaction. It is thus indicated that the reaction of wet oxidants is promoted by O₂ molecules when both dry and wet oxidants are closely located at the SiO₂/4H–SiC(000 $\bar{1}$) interface. Although further calculations are necessary to clarify how the reactions continue to promote the oxide growth, the

TABLE I. Final atomic configuration, calculated reaction energy E_{rc} , and barrier heights E_b of the interfacial reaction at $\text{SiO}_2/4\text{H-SiC}$ interfaces for various oxidizing species. The calculated E_b for single O_2 and H_2O molecules and OH groups at $\text{SiO}_2/4\text{H-SiC}$ interfaces obtained in previous calculations in Refs. [35,36] are also shown for comparison. Note that the reactions of single H_2O molecule and OH group at $\text{SiO}_2/\text{SiC}(0001)$ interface are endothermic. Details of the reactions of wet oxidant are described in Ref. [36]. The calculated results for the $\text{O}_2 + \text{H}_2\text{O}$ and $\text{O}_2 + \text{OH}$ reactions at $\text{SiO}_2/\text{SiC}(0001)$ interface and for the $\text{O}_2 + \text{OH}$ and $\text{O}_2 + 2\text{OH}$ reactions at $\text{SiO}_2/\text{SiC}(000\bar{1})$ interface are described in Ref. [69].

Orientation	Oxidants	Final atomic configuration	E_{rc} (eV)	E_b (eV)
(0001)	O_2	$\text{Si-O-Si} + \text{CO}$	0.99 ^a	3.2 ^a
	2OH	$\text{Si-O-Si} + \text{CH-OH}$	2.91 ^b	2.24 ^b
	$\text{O}_2 + \text{H}_2\text{O}$	$\text{Si-H} + \text{Si-O-H} + 2\text{Si-O-Si} + \text{CO}$	1.19 ^c	2.65 ^c
	$\text{O}_2 + \text{OH}$	$\text{Si-H} + \text{Si}_3\text{-O} + \text{CO}_2$	3.89 ^c	3.18 ^c
	$\text{O}_2 + 2\text{OH}$	$\text{Si-H} + \text{Si}_3\text{-O} + \text{Si-O-H} + \text{CO}_2$	7.08	1.63
	O_2	$\text{Si-O-Si} + \text{CO}$	4.56 ^a	2.4 ^a
(000 $\bar{1}$)	H_2O	$\text{Si-O-CH}_2\text{-C} + \text{Si-O-C}$	2.07 ^b	2.2 ^b
	OH	$\text{Si-O-CH-C} + \text{Si-O-Si}$	2.35 ^b	2.2 ^b
	2OH	$\text{C-C=O} + \text{Si-O-H} + \text{C-H} + \text{Si-O-Si} + \text{Si-O-C}$	4.73 ^b	2.5 ^b
	$\text{O}_2 + \text{H}_2\text{O}$	$\text{Si-O-CH}_2\text{-C} + \text{CO}_2$	8.25	1.51
	$\text{O}_2 + \text{OH}$	$\text{Si-O-CH-C} + \text{CO}_2$	8.0 ^c	1.40 ^c
	$\text{O}_2 + 2\text{OH}$	$\text{Si-O-H} + \text{C-H} + \text{CO} + \text{CO}_2$	10.50 ^c	1.48 ^c

^aReference [35].

^bReference [36].

^cReference [69].

presence of many topmost carbon lattice sites of SiC shown in Fig. 4(b) suggests that the promotion proceeds after the reaction obtained by present study. From the viewpoint of defect generation at the interface, a C-C bond is formed as shown in Fig. 4(b). However, our inspection of calculated wave functions clarifies that there are no localized electronic states caused by the C-C bond in the energy gap of SiC. This is because H atoms contribute to terminating the dangling bonds of the C atom in C-C configuration. The passivation by H atoms is effective for reducing D_{it} , but the presence of many H atoms at the interface might lead to an intrinsic problem related to gate oxide reliability such as the reduction of breakdown voltage [19].

C. Orientation and wet oxidation condition dependence

In this subsection, we discuss the orientation dependence of interfacial reaction by the coexistence of dry and wet ambients in comparison with those by single dry and wet oxidations. Table I summarizes the final atomic configurations, calculated reaction energies E_{rc} , and barrier heights E_b for the interfacial reactions obtained in this study, along with those in previous calculations [35,36]. It is found that gas-phase carbon oxides such as CO_2 are generated as a resultant structure after the interfacial reaction regardless of the interface orientation. For the $\text{SiO}_2/4\text{H-SiC}(0001)$ interface, the calculated barrier height for the $\text{O}_2 + \text{H}_2\text{O}$ reaction is lower than that of O_2 molecule. Moreover, the barrier height for the $\text{O}_2 + 2\text{OH}$ reaction (1.63 eV) is lower than those of the O_2 molecule (3.2 eV) and two OH groups (2.24 eV). Since the energy of the initial structure for the $\text{O}_2 + \text{H}_2\text{O}$ ($\text{O}_2 + 2\text{OH}$) reaction is lower (higher) than the sum of total energies of initial structures for the O_2 and H_2O (2OH) reactions by only 0.22 (0.08) eV [72], the stability of initial structures is negligible at high temperatures and the preferable reaction for coexisting oxidant compared with the specific one

is simply determined by comparing the energy barriers. Judging from the barrier heights of the reactions, the $\text{O}_2 + \text{H}_2\text{O}$ ($\text{O}_2 + 2\text{OH}$) reaction, in which H_2O molecule (OH group) is initially incorporated as Si-OH (C-OH) bonds, preferably occurs when O_2 and H_2O (2OH) coexist at the interface. By comparing the barrier heights shown in Table I, the lowest barrier height (1.63 eV) is obtained in the $\text{O}_2 + 2\text{OH}$ reaction. However, to determine whether the $\text{O}_2 + \text{H}_2\text{O}$ or $\text{O}_2 + 2\text{OH}$ reaction is dominant, detailed analysis of the rate constant in the Deal-Grove model [45] considering the formation OH groups from H_2O is necessary, as we discuss later.

In contrast, the calculated barrier heights E_b for the reaction O_2 molecule including wet oxidants at the $\text{SiO}_2/4\text{H-SiC}(000\bar{1})$ interface are lower than those of the single oxidation processes by dry and wet ambients. This is because the barrier heights of the H_2O molecule and OH groups become lower, owing to the presence of the O_2 molecule, as described in Sec. III B. According to the calculated E_b in Table I, it seems that each combination of dry and wet oxidizing species equally contributes to the interfacial reaction. However, the concentrations of OH groups in SiO_2 is expected to be lower than that of H_2O molecules due to the energy of the OH group in SiO_2 being higher than that of the H_2O molecule [66,67]. It is thus expected that the O_2 reaction with H_2O mainly contributes to the promotion of interfacial reaction at the $\text{SiO}_2/4\text{H-SiC}(000\bar{1})$ interface. The calculated barrier heights shown in Table I manifest that the coexistence of dry and wet ambients is crucial for the promotion of the interfacial oxidation processes on both $\text{SiO}_2/4\text{H-SiC}(0001)$ and $(000\bar{1})$ interfaces, although the dominant reaction pathways depend on the orientation.

Furthermore, to clarify significant enhancement of the growth rate by the coexistence of dry and wet oxidants, the linear rate constants in the Deal-Grove model [45] are evaluated by using the barrier heights of each reaction pathway shown in Table I. The linear rate constant $dX/dt = B/A$ at

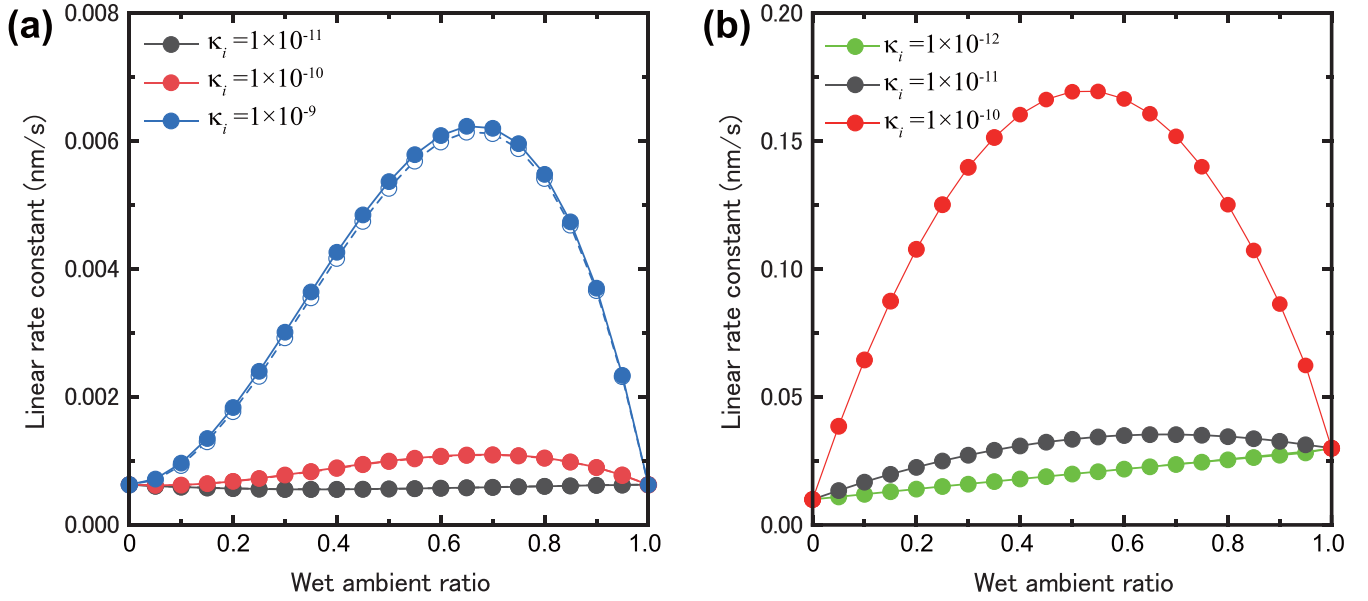


FIG. 6. Calculated linear rate constant in the Deal-Grove model at 1400 K using Eq. (1) at (a) $\text{SiO}_2/4\text{H-SiC}(0001)$ and (b) $(000\bar{1})$ interfaces as a function of wet ambient ratio r_{wet} . Open circles with dashed lines at $\text{SiO}_2/4\text{H-SiC}(0001)$ interface represent the linear rate constant without the contribution of $\text{O}_2 + \text{H}_2\text{O}$ reaction. The parameters values of κ_i for coexisting oxidants are ranging from 1×10^{-11} to 1×10^{-9} at $\text{SiO}_2/4\text{H-SiC}(0001)$ interface and from 1×10^{-12} to 1×10^{-10} at $\text{SiO}_2/4\text{H-SiC}(000\bar{1})$ interface. Note that the rate constants with the contribution of $\text{O}_2 + \text{H}_2\text{O}$ reaction overlap those without the contribution of $\text{O}_2 + \text{H}_2\text{O}$ reaction for $\kappa_i = 1 \times 10^{-11}$ and 1×10^{-10} .

temperature T for the reaction of O_2 molecules including wet oxidants is expressed by the sum of linear rate constants for each reaction pathway as

$$\frac{dX}{dt} = \frac{B}{A} \approx \sum_i \frac{C_{\text{ox}}^i}{N_{\text{ox}}} \frac{\kappa_i k_B T}{h} \exp\{-E_b^i/k_B T\}, \quad (1)$$

where X is oxide thickness, B/A is the linear rate constant, h is the Planck's constant, k_B is the Boltzmann's constant, C_{ox}^i , κ_i , and E_b^i are the equilibrium concentration, transmission coefficient, and barrier height for i th reaction pathway shown in Table I, respectively. Note that the dissociation of weak bonds between OH groups and Si atoms of SiO_2 near the interface are incorporated in E_b^i for the reactions including OH groups. We employ the solubilities of O_2 and H_2O molecules (5.2×10^{16} and $3.0 \times 10^{19} \text{ cm}^{-3}$, respectively) for C_{ox}^i of the O_2 and H_2O reactions [45]. The value of C_{ox}^i for single OH group ($4.0 \times 10^{17} \text{ cm}^{-3}$) is estimated by considering the dissociation probability of H_2O , which is determined from the formation energies of OH groups from H_2O and two H_2O molecules ($\sim 0.5 \text{ eV}$) in Refs. [66,67]. Since direct calculations of C_{ox}^i for the 2OH , $\text{O}_2 + \text{H}_2\text{O}$, $\text{O}_2 + \text{OH}$, and $\text{O}_2 + 2\text{OH}$ reactions are difficult, we numerically estimate the effective concentrations of coexisting oxidants by counting the numbers of oxidizing species in which the distance between neighboring oxidants is less than 10 \AA . The distance of 10 \AA is determined from the initial-state structures for the reaction pathways shown in Figs. 1(a) and 4(a). The positions of each oxidant satisfying its equilibrium concentration are randomly distributed in the periodic unit cell with the size of $500 \times 500 \times 500 \text{ nm}$ and averaged values of the numbers of oxidant pairs (for the 2OH , $\text{O}_2 + \text{H}_2\text{O}$, $\text{O}_2 + \text{OH}$ reactions) and triplets (for the $\text{O}_2 + 2\text{OH}$ reaction) whose distances are less than 10 \AA are obtained by 50 samples with different

atomic configurations. $N_{\text{ox}} = 4.5 \times 10^{22} \text{ cm}^{-3}$ is the number of oxidant molecules incorporated into a unit volume of SiO_2 . In the case of the incorporation of two O atoms after the reaction, such as the $\text{O}_2 + \text{OH}$ and $\text{O}_2 + 2\text{OH}$ reactions at the $\text{SiO}_2/4\text{H-SiC}(000\bar{1})$ interface, $N_{\text{ox}} = 2.25 \times 10^{22} \text{ cm}^{-3}$ is used. In this paper, the interfacial reaction rate in the Deal-Grove model for each reaction pathway, k_i , is expressed by the Eyring equation written as $k_i = \frac{\kappa_i k_B T}{h} \exp\{-E_b^i/k_B T\}$. We here note that the contribution of activation entropy is involved in the transmission coefficient. For the $\text{SiO}_2/4\text{H-SiC}(0001)$ interface, the values of $\kappa_i = 9 \times 10^{-8}$ (4×10^{-12}) for the O_2 (2OH) reaction are obtained to reproduce the experimentally reported oxide growth rate in Refs. [25,26]. Similarly, the values of $\kappa_i = 1.2 \times 10^{-9}$ (1.3×10^{-12}) for the O_2 (H_2O) reaction is obtained to reproduce the growth rate of dry oxidation in Ref. [40] and three times larger oxide thickness in wet oxidation compared with the thickness in dry oxidation in Ref. [46] at the $\text{SiO}_2/4\text{H-SiC}(000\bar{1})$ interface. The transmission coefficients for coexisting oxidants are parameterized ranging from $\kappa_0 = 1 \times 10^{-12}$ to 1×10^{-9} irrespective of the form of coexisting oxidants. Figure 6 shows the calculated linear rate constants at $T = 1400 \text{ K}$ using Eq. (1) as a function of wet ambient ratio r_{wet} at the $\text{SiO}_2/4\text{H-SiC}(0001)$ and $(000\bar{1})$ interfaces. Here, the wet ambient ratio r_{wet} is given by the ratio of H_2O partial pressure with respect to the sum of H_2O pressure and O_2 pressure. The calculated linear rate constants successfully reproduce the orientation dependence in the growth rate. The linear rate constant at the $\text{SiO}_2/4\text{H-SiC}(0001)$ interface shown in Fig. 6(a) is much smaller than that at the $\text{SiO}_2/4\text{H-SiC}(000\bar{1})$ interface shown in Fig. 6(b). When the values of κ_i are larger than 1×10^{-10} and 1×10^{-11} for $\text{SiO}_2/4\text{H-SiC}(0001)$ and $(000\bar{1})$ interfaces, respectively, the rate constants do not increase monotonically with r_{wet} .

This trend is quite different from Si oxidation by the mixture of dry and wet ambients [47].

For the SiO₂/4H-SiC(0001) interface, it is found that the maximum of the linear rate constant in Fig. 6(a) is located at $r_{\text{wet}} = 0.65$ for κ_i larger than 1×10^{-10} . Moreover, the enhancement of the rate constant for $r_{\text{wet}} \geq 0.65$ is predominant compared with that for $r_{\text{wet}} \leq 0.65$. This is because the O₂ + 2OH reaction is dominant at the SiO₂/4H-SiC(0001) interface. The ratio dependence of the linear rate constant corresponds to the behavior of C_{ox}^i for the O₂ + 2OH reaction with respect to the wet ambient ratio. Even though the amount of C_{ox}^i for the O₂ + 2OH reaction is quite small, less than $6 \times 10^{13} \text{ cm}^{-3}$, the O₂ + 2OH reaction is more activated than those with the H₂O molecule and single OH group, owing to its low barrier height (1.63 eV) at the SiO₂/4H-SiC(0001) interface. It should be noted that the O₂ + H₂O reaction hardly contributes to the linear rate constant, as seen in the open circles of Fig. 6(a). If we allow for the relatively large value in κ_i for the O₂ + 2OH reaction, the trend of calculated linear rate constant is qualitatively consistent with experiments: Recent experimental observations for the SiO₂/4H-SiC(0001) interface have reported that the favorable condition for oxide growth rate is H₂O : O₂ = 6 : 4 in partial pressure [25,26]. It should be noted that the calculated barrier height of 1.63 eV for the O₂ + 2OH reaction reasonably agrees with the experimentally reported activation energy estimated by oxide growth rate (1.3 eV) [25,26].

As mentioned in Sec. III B, the barrier heights of both the H₂O molecule and OH groups are reduced by coexisting with O₂ molecule at the SiO₂/4H-SiC(000 $\bar{1}$) interface. Therefore, the O₂ + H₂O reaction is most likely to occur due to similar barrier heights of coexisting oxidants ranging from 1.45 to 1.51 eV and small C_{ox}^i in the O₂ + OH and O₂ + 2OH reactions compared with C_{ox}^i of the O₂ + H₂O reaction. As seen in Fig. 6(b), the maximum of the rate constant is located at $r_{\text{wet}} = 0.55$ for $\kappa_i = 1 \times 10^{-10}$. On the other hand, the maximum of the rate constant is located at $r_{\text{wet}} = 0.7$ for $\kappa_i = 1 \times 10^{-11}$. The difference depending on the value of κ_i is caused by the difference in the linear rate constant between $r_{\text{wet}} = 0$ and 1. If the contribution of the O₂ + H₂O reaction becomes dominant compared with the rate constant difference between $r_{\text{wet}} = 0$ and 1, the maximum of the rate constant is located at $0.5 \leq r_{\text{wet}} \leq 0.55$. This situation is realized for $\kappa_i \geq 3 \times 10^{-11}$. The presence of the maximum in the linear rate constant for $\kappa_i \geq 1 \times 10^{-11}$ at the SiO₂/4H-SiC(000 $\bar{1}$) interface is qualitatively consistent with the experimental results of maximum oxide thickness [46]. Owing to the difference in the dominant reaction pathway depending on the plane orientation, it is suggested that the optimal wet ambient condition at the SiO₂/4H-SiC(0001) interface is different from that at the SiO₂/4H-SiC(000 $\bar{1}$) interface.

Furthermore, we comment on the temperature dependence of the optimal wet condition ranging from 1300 to 1500 K. When κ_i for dominant reaction pathways are larger than 2×10^{-10} and 4×10^{-11} , the maximum of rate constants at $1300 \leq T \leq 1500 \text{ K}$ is located at $r_{\text{wet}} = 0.65$ and 0.55 at the SiO₂/4H-SiC(0001) and (000 $\bar{1}$) interfaces, respectively. This is because the linear rate constants uniformly increase with temperature owing to the Boltzmann factor in Eq. (1).

Although the effect of transmission coefficients of coexisting oxidants should be carefully examined, it is implied that the value of r_{wet} with the largest rate constant is insensitive to temperature.

IV. CONCLUSIONS

We have investigated the reaction mechanism of an O₂ molecule including H₂O molecule and OH groups at SiO₂/4H-SiC interface by performing systematic *ab initio* calculations. Our *ab initio* calculations using slab models to simulate the SiO₂/4H-SiC interface away from the oxide surface have revealed characteristic features of the concerted reactions by dry and wet oxidants within density functional theory. For the SiO₂/4H-SiC(0001) interface, the reactions of wet oxidants such as H₂O molecules including O₂ molecules are different from those of simple wet oxidation processes. The dissociation of H₂O molecules is triggered by coexisting O₂ molecule, leading to the promotion of interfacial reaction as well as the stabilization of the interface structures. On the other hand, the H₂O molecule easily reacts at the SiO₂/4H-SiC(000 $\bar{1}$) interface by the coexisting O₂ molecule. The calculated barrier heights for the O₂ + H₂O reaction are much lower than those of the single oxidation processes by dry and wet oxidants, indicating the promotion of interfacial reaction at the SiO₂/4H-SiC(000 $\bar{1}$) interface. We have furthermore evaluated the linear rate constants in the Deal-Grove model at the SiO₂/4H-SiC(0001) and (000 $\bar{1}$) interfaces to elucidate the wet oxidation condition dependence. On the basis of estimated linear rate constants using the results of *ab initio* calculations and experimentally reported solubilities and reaction rates for dry and wet oxidations, we have found that the optimal wet ambient condition at the SiO₂/4H-SiC(0001) interface is different from that at the SiO₂/4H-SiC(000 $\bar{1}$) interface. This is because of the difference in active oxidants under wet oxidation conditions between SiO₂/4H-SiC(0001) and (000 $\bar{1}$) interfaces. The trend of wet oxidation conditions obtained by the present study is qualitatively consistent with experimentally reported oxide growth rates. Although effects of disordered structure of SiO₂ and intrinsic defects in the SiC side of the interface as well as those in SiO₂ should be carefully examined, the calculated results offer better understanding of the atom-scale mechanisms as well as the origin of the significant enhancement of interfacial reaction by the coexistence of dry and wet oxidants.

ACKNOWLEDGMENTS

This work was supported by JSPS KAKENHI Grants No. JP16H06418, No. JP19K05268, and No. JP20K05324, CREST-JST Grant No. JPMJCR16N2, and the Collaborative Research Program of Research Institute for Applied Mechanics at Kyushu University. The computations were performed using computing facilities at the Research Center for Computational Science (National Institutes of Natural Sciences) and Research Institute for Information Technology (Kyushu University).

- [1] N. S. Saks, S. S. Mani, and A. K. Agarwal, *Appl. Phys. Lett.* **76**, 2250 (2000).
- [2] V. V. Afanasev, M. Bassler, G. Pensl, and M. Schulz, *Phys. Status Solidi A* **162**, 321 (1997).
- [3] L. Muehlhoff, M. J. Bozack, W. J. Choyke, and J. T. Yates, *J. Appl. Phys.* **60**, 2558 (1986).
- [4] A. Suzuki, H. Ashida, N. Furui, K. Mameno, and H. Matsunami, *Jpn. J. Appl. Phys.* **21**, 579 (1982).
- [5] Y. Song, S. Dhar, L. C. Feldman, G. Chung, and J. R. Williams, *J. Appl. Phys.* **95**, 4953 (2004).
- [6] T. Yamamoto, Y. Hijikata, H. Yaguchi, and S. Yoshida, *Jpn. J. Appl. Phys.* **46**, L770 (2007).
- [7] T. Yamamoto, Y. Hijikata, H. Yaguchi, and S. Yoshida, *Jpn. J. Appl. Phys.* **47**, 7803 (2008).
- [8] E. A. Ray, J. Rozen, S. Dhar, L. C. Feldman, and J. R. Williams, *J. Appl. Phys.* **103**, 023522 (2008).
- [9] S. Kumar and J. Alhar, in *Silicon Carbide Materials, Processing and Application in Electronic Devices*, edited by M. Mukherjee (InTech, Rijeka, 2011).
- [10] D. Goto, Y. Hijikata, S. Yagi, and H. Yaguchi, *J. Appl. Phys.* **117**, 095306 (2015).
- [11] T. Hosoi, D. Nagai, T. Shimura, and H. Watanabe, *Jpn. J. Appl. Phys.* **54**, 098002 (2015).
- [12] T. Hosoi, D. Nagai, M. Sometani, Y. Katsu, H. Takeda, T. Shimura, M. Takei, and H. Watanabe, *Appl. Phys. Lett.* **109**, 182114 (2016).
- [13] Z. Zheng, R. E. Tressler, and K. E. Spear, *J. Electrochem. Soc.* **137**, 854 (1990).
- [14] K. Fukuda, M. Kato, K. Kojima, and J. Senzaki, *Appl. Phys. Lett.* **84**, 2088 (2004).
- [15] J. N. Shenoy, M. K. Das, J. A. Cooper, M. R. Melloch, and J. W. Palmour, *J. Appl. Phys.* **79**, 3042 (1996).
- [16] M. Okamoto, Y. Makifuchi, M. Iijima, Y. Sakai, N. Iwamoto, H. Kimura, K. Fukuda, and H. Okumura, *Appl. Phys. Express* **5**, 041302 (2012).
- [17] R. H. Kikuchi and K. Kita, *Appl. Phys. Lett.* **104**, 052106 (2014).
- [18] R. H. Kikuchi and K. Kita, *Appl. Phys. Lett.* **105**, 032106 (2014).
- [19] E. D. Indari, Y. Yamashita, R. Hasunuma, H. Oji, and K. Yamabe, *AIP Adv.* **9**, 105018 (2019).
- [20] R. Kosugi, S. Suzuki, M. Okamoto, S. Harada, J. Senzaki, and K. Fukuda, *IEEE Electron Devices Lett.* **23**, 136 (2002).
- [21] T. Narushima, T. Goto, and T. Hirai, *J. Am. Ceram. Soc.* **72**, 1386 (1989).
- [22] H. Hirai and K. Kita, *Appl. Phys. Lett.* **103**, 132106 (2013).
- [23] H. Hirai and K. Kita, *Appl. Phys. Express* **8**, 021401 (2015).
- [24] H. Hirai and K. Kita, *Appl. Phys. Lett.* **110**, 152104 (2017).
- [25] K. Kita, H. Hirai, and K. Ishinoda, *ECS Trans.* **80**, 123 (2017).
- [26] K. Kita, H. Hirai, H. Kajifusa, K. Kuroyama, and K. Ishinoda, *Microelectron. Eng.* **178**, 186 (2017).
- [27] K. Kita, R. H. Kikuchi, and H. Hirai, *ECS Trans.* **61**, 135 (2014).
- [28] Y. Kagoyama, M. Okamoto, T. Yamasaki, N. Tajima, J. Nara, T. Ohno, H. Yano, S. Harada, and T. Umeda, *J. Appl. Phys.* **125**, 065302 (2019).
- [29] F. Devynck, F. Giustino, and A. Pasquarello, *Microelectron. Eng.* **80**, 38 (2005).
- [30] F. Devynck, F. Giustino, P. Broqvist, and A. Pasquarello, *Phys. Rev. B* **76**, 075351 (2007).
- [31] T. Ohmura, A. Miyashita, M. Iwasaka, M. Yoshikawa, and H. Tsuchida, *Mater. Sci. Forum* **556**, 615 (2007).
- [32] E. Okuno, T. Sakakibara, S. Onda, M. Itoh, and T. Uda, *Appl. Phys. Express* **1**, 061401 (2008).
- [33] X. Shen, B. R. Tuttle, and S. T. Pantelides, *J. Appl. Phys.* **114**, 033522 (2013).
- [34] K. Chokawa, S. Kato, K. Kamiya, and K. Shiraishi, *Mater. Sci. Forum* **740**, 469 (2013).
- [35] T. Akiyama, A. Ito, K. Nakamura, T. Ito, H. Kageshima, M. Uematsu, and K. Shiraishi, *Surf. Sci.* **641**, 174 (2015).
- [36] T. Akiyama, S. Hori, K. Nakamura, T. Ito, H. Kageshima, M. Uematsu, and K. Shiraishi, *Jpn. J. Appl. Phys.* **57**, 04FR08 (2018).
- [37] T. Shimizu, T. Akiyama, A.-M. Pradipto, K. Nakamura, T. Ito, H. Kageshima, M. Uematsu, and K. Shiraishi, *Jpn. J. Appl. Phys.* **59**, SMMD01 (2020).
- [38] T. Shimizu, T. Akiyama, K. Nakamura, T. Ito, H. Kageshima, M. Uematsu, and K. Shiraishi, *ECS Trans.* **98**, 37 (2020).
- [39] Z. Zhang, Z. Wang, Y. Guo, and J. Robertson, *Appl. Phys. Lett.* **118**, 031601 (2021).
- [40] Y. Hijikata, H. Yaguchi, and S. Yoshida, *Appl. Phys. Express* **2**, 021203 (2009).
- [41] D. Goto and Y. Hijikata, *J. Phys. D* **49**, 225103 (2016).
- [42] S. Takamoto, T. Yamasaki, T. Ohno, C. Kaneta, A. Hatano, and S. Izumi, *J. Appl. Phys.* **123**, 185303 (2018).
- [43] C. I. Harris and V. V. Afanasev, *Microelectron. Eng.* **36**, 167 (1997).
- [44] I. Vickridge, J. Ganem, Y. Hoshino, and I. Trimaille, *J. Phys. D* **40**, 6254 (2007).
- [45] B. E. Deal and A. S. Grove, *J. Appl. Phys.* **36**, 3770 (1965).
- [46] M. Okamoto, Y. Makifuchi, T. Araoka, M. Miyazato, Y. Sugahara, T. Tsutsumi, Y. Onishi, H. Kimura, S. Harada, K. Fukuda, A. Otsuki, and H. Okumura, *Mater. Sci. Forum* **778**, 975 (2014).
- [47] W. Lerch, G. Roters, P. Münzinger, R. Mader, and R. Ostermeir, *Mater. Sci. Eng. B* **54**, 153 (1998).
- [48] In the slab models, an artificial electric field (~ 1.25 eV) is induced by hydrogen passivation of the top and bottom layers. However, the field hardly affects the reaction energies. The differences in the reaction energies with and without dipole correction [L. Bengtsson, *Phys. Rev. B* **59**, 12301 (1999)] are found to be less than 0.06 eV.
- [49] K. Shiraishi, K. Chokawa, H. Shirakawa, K. Endo, M. Araidai, K. Kamiya, and H. Watanabe, in *Proceedings of the 2014 IEEE International Electron Devices Meeting (IEEE, Piscataway, NJ, 2014)*, pp. 21.3.1–21.3.4.
- [50] T. Kobayashi and Y.-I. Matsushita, *J. Appl. Phys.* **126**, 145302 (2019).
- [51] Al.-M. El-Sayed, Y. Wimmer, W. Goes, T. Grasser, V. V. Afanasev, and A. L. Shluger, *Microelectron. Eng.* **147**, 141 (2015).
- [52] Al.-M. El-Sayed, Y. Wimmer, W. Goes, T. Grasser, V. V. Afanasev, and A. L. Shluger, *Phys. Rev. B* **92**, 014107 (2015).
- [53] M. S. Munde, D. Z. Gao, and Alexander L Shluger, *J. Phys.: Condens. Matter* **29**, 245701 (2017).
- [54] M. V. Mistry, J. Cottom, K. Patel, A. L. Shluger, G. C. Sosso, and G. Pobegen, *Modelling Simul. Mater. Sci. Eng.* **29**, 035008 (2021).
- [55] T. Akiyama and H. Kageshima, *Surf. Sci.* **576**, L65 (2005).

- [56] A. Bongiorno and A. Pasquarello, *Phys. Rev. Lett.* **93**, 086102 (2004).
- [57] Y. Yoshimoto and S. Tsuneyuki, *Surf. Sci.* **514**, 200 (2002).
- [58] J. Yamauchi, Y. Yoshimoto, and Y. Suwa, *Appl. Phys. Lett.* **99**, 191901 (2011).
- [59] J. P. Perdew, K. Burke, and M. Ernzerhof, *Phys. Rev. Lett.* **77**, 3865 (1996).
- [60] N. Troullier and J. L. Martins, *Phys. Rev. B* **43**, 1993 (1991).
- [61] D. Vanderbilt, *Phys. Rev. B* **41**, 7892 (1990).
- [62] J. Yamauchi, M. Tsukada, S. Watanabe, and O. Sugino, *Phys. Rev. B* **54**, 5586 (1996).
- [63] H. Kageshima and K. Shiraishi, *Phys. Rev. B* **56**, 14985 (1997).
- [64] Y. Zhang and W. Yang, *Phys. Rev. Lett.* **80**, 890 (1998).
- [65] K. M. Davis and M. Tomozawa, *J. Non-Cryst. Solids* **201**, 177 (1996).
- [66] T. Bakos, S. N. Rashkeev, and S. T. Pantelides, *Phys. Rev. Lett.* **88**, 055508 (2002).
- [67] T. Bakos, S. N. Rashkeev, and S. T. Pantelides, *Phys. Rev. B* **69**, 195206 (2004).
- [68] G. Henkelman, *J. Chem. Phys.* **113**, 9901 (2000).
- [69] See Supplemental Material at <https://link.aps.org/supplemental/10.1103/PhysRevMaterials.5.114601> for the calculated results of the reactions for O₂, including H₂O and O₂, including single OH group at the SiO₂/4H-SiC(0001) interface and those for O₂, including single OH group and O₂, including two OH groups at the SiO₂/4H-SiC(0001) interface.
- [70] Y. Kangawa, T. Ito, Y. S. Hiraoka, A. Taguchi, K. Shiraishi, and T. Ohachi, *Surf. Sci.* **507-510**, 285 (2002).
- [71] Although the main contribution of energy gains (Si–O bond formation) from C to E in Fig. 2(b) is the same as that from E to G in Fig. 5(a), the energy gain from C to E in Fig. 2(b) is larger than that from E to G in Fig. 5(a) by 1.9 eV. This is because the energy of metastable structures are different with each other.
- [72] The relative stability of initial structures is evaluated by the energy difference $\Delta E = E_{\text{O}_2+\text{H}_2\text{O}} + E_{\text{int}} - E_{\text{O}_2} - E_{\text{H}_2\text{O}} = 0.08$ eV for the O₂ + H₂O reaction and $\Delta E = E_{\text{O}_2+2\text{OH}} + E_{\text{int}} - E_{\text{O}_2} - E_{2\text{OH}} = -0.22$ eV for the O₂ + 2OH reaction, where $E_{\text{O}_2+\text{H}_2\text{O}}$, $E_{\text{O}_2+2\text{OH}}$, E_{O_2} , $E_{\text{H}_2\text{O}}$, and $E_{2\text{OH}}$ are the total energies of the initial structures for the O₂ + H₂O, O₂ + 2OH, O₂, H₂O, and 2OH reactions, respectively, and E_{int} is the total energy of interface without oxidants.